



Research Paper

Coral-inferred historical changes of nickel emissions related to industrial and transportation activities in the Beibu Gulf, northern South China Sea

Xingyuan Wu^a, Wei Jiang^{a,b,*}, Kefu Yu^{a,b,*}, Shendong Xu^{a,b}, Haodan Yang^a, Ning Wang^a, Chaoshuai Wei^a, Chunmei Feng^a, Yinan Sun^a, Sirong Xie^{a,c}^a Guangxi Laboratory on the Study of Coral Reefs in the South China Sea, School of Marine Sciences, Guangxi University, Nanning 530004, PR China^b Southern Marine Science and Engineering Guangdong Laboratory (Zhuhai), Zhuhai 519080, PR China^c School of Resources, Environment and Materials, Guangxi University, Nanning 530004, PR China

ARTICLE INFO

Editor: Dr. C. LingXin

Keywords:

Nickel
South China Sea
Coral
Weizhou Island
Oil spills

ABSTRACT

As one of the most abundant metals in heavy oils, Ni has suffered so notably increasing impacts from industrial and traffic activities that anthropogenic Ni emissions have altered natural geochemical processes. The coral Ni/Ca has become a reliable proxy for characterizing marine pollution, but this potential has been unexploited for highlighting oil pollution. Here, we utilized a high-resolution record of geochemical parameters (Ni/Ca, $\delta^{18}\text{O}$, and $\delta^{13}\text{C}$) in a *Porites* coral of an offshore island in the northern South China Sea to reconstruct of Ni distribution patterns in surface seawater from 1984 to 2015. The coral Ni/Ca ratios exhibit minor fluctuations, except for multiple mutation peaks ($0.20 \pm 0.42 \mu\text{mol/mol}$) during the period from 1984 to 1993. The ratio was low and stable ($0.10 \pm 0.09 \mu\text{mol/mol}$) from 1994 to 2008, and then increased rapidly with significant variations ($1.60 \pm 4.56 \mu\text{mol/mol}$) from 2009 to 2015. The coral Ni/Ca ratios captured all significant Ni discharges, and this demonstrates its potential for recording oil spill episodes. The historical variations in the contributions of Ni indicate that industrial and traffic activities should be responsible for changes in the anthropogenic input. The leaks and consumptions of petroleum likely account for the primary Ni emission sources.

1. Introduction

Nickel (Ni) is a transition metal, which acts as a bio-limiting micronutrient for marine microorganisms at the surfaces of oceans, and thus, it significantly influences enzyme activities in marine phytoplankton (Aciego et al., 2015; Mackey et al., 2002; Sunda, 1989). Its residence time in the ocean of approximately 1340 ± 690 a (Kadko et al., 2019) between those of conservative and active elements. A significant imbalance exists between its input to the ocean and the associated output: the sedimentary inputs are considerably lower than the outputs (Gaillardet et al., 2003; Li and Schoonmaker, 2003). In the open ocean, the concentration of Ni generally varies between 2 and 4 nmol/kg in the surface water and between 5 and 12 nmol/kg in the deep water, with a global average of ~ 8.2 nmol/kg (Archer et al., 2020; Dupont et al., 2009; Mackey et al., 2002; MBARI, 2012; Takano et al., 2017). Comprehending long-term variations in the concentration of Ni in seawater is significant for tracking the evolution of the biosphere and understanding environmental dynamics including climate change. However,

conventional approaches (e.g., sediment core) used for the assessment of Ni in the ocean generally involve a low resolution (Amorosi, 2012). Consequently, a continuous high-resolution Ni record for the ocean is unavailable, and this hinders the understanding of its dynamics in the ocean and the association to global climate change.

In addition to their utility for the extraction of resources, reef corals in tropical seas enable quantification of ancient and modern environmental changes in the ocean (Lough, 2010; Xu et al., 2021). In fact, compared to conventional media, coral reefs with the properties of high-resolution, high-precision, easy dating, a closed system, relatively complete records, etc., can provide more detailed information on changes in the ocean (Gagan et al., 2000; Yu et al., 2005). Owing to the higher concentrations of metals in coral compared to primitive seawater, coral metal/Ca ratios have been employed as tracers of different metals in the marine environment. Based on *Porites* collected from Sabah (Malaysia), the distribution coefficient $((\text{Metal}/\text{Ca})_{\text{coral}}/(\text{Metal}/\text{Ca})_{\text{seawater}})$ of Ni in coral is ~ 0.59 (Mokhtar et al., 2012). In fact, the Ni/Ca ratio obtained using coralline red algae revealed the different stages of

* Correspondence to: School of Marine Sciences, Guangxi University, Nanning 530004, PR China.

E-mail addresses: jianwe@gxu.edu.cn (W. Jiang), kefuyu@scsio.ac.cn (K. Yu).<https://doi.org/10.1016/j.jhazmat.2021.127422>

Received 22 July 2021; Received in revised form 24 September 2021; Accepted 1 October 2021

Available online 5 October 2021

0304-3894/© 2021 Elsevier B.V. All rights reserved.

mining activities in New Caledonia (Nicolas et al., 2018). However, studies on Ni in coral reefs have focused on its potential negative effects on corals, rather than its utility as a proxy for pollution (Ali et al., 2011; Gillmore et al., 2020; Gissi et al., 2019; Jayaraju et al., 2009).

Although Vanadium(V) and Ni are both commonly abundant in heavy oils, but the existing studies on tracing petroleum pollution usually employ the V/Ca ratio of corals, while the Ni/Ca is neglected (Bastidas and Garcia, 1999; Guzmán and Carlos, 1992; Guzmán and Jarvis, 1996). Generally, V dominates in sulfur-rich petroleum, while Ni is prevalent in low-sulfur and high-nitrogen petroleum (Dechaine and Gray, 2010; López and Lo Mónaco, 2017). In China, crude oil is commonly low-sulfur and contains higher Ni relative to V because of their origin from terrestrial organisms (Zhao et al., 2015), and thus, the coral Ni/Ca ratio is a potential proxy for tracing oil pollution in Chinese waters. The combustion of fossil fuels, oil field development and leakage from oil tankers represent major anthropogenic sources of dissolved Ni in seawater (Alharbi et al., 2017). During oil field development, for example, the risk of oil spills of varying magnitudes exists at different stages, and the Ni involved can be released to the seawater column through bacterial decomposition and oil dissolution, and then deposited on marine sediments (Cantú et al., 2000; Liu et al., 2015; Santos-Echeandía et al., 2005, 2008). In addition, because Ni is among the most abundant trace metals in ship fuel oils, it is increasingly exploited as a tracer of ship emissions (Celo et al., 2015; Corbin et al., 2018). Zhao et al. (2021) reported that ship emissions contributed approximately 40% of Ni released in most coastal regions in East Asia. Ni emitted to the atmosphere commonly remains near the source vessel, and subsequently dissolves in the surface seawater (Endres et al., 2018), which under appropriate conditions is incorporated into coral skeletons.

The Weizhou Island (WZI) in the northern South China Sea (SCS) is an ideal area for evaluating the utility of the Ni/Ca ratio of corals for reconstructing pollution events. This is because the WZI is a touristic island for which environmental and climatic data that can be used for validation of the of coral records are available. In addition, many coral reefs are developing in the WZI, and these record surface seawater Ni concentrations, which can be unraveled using high-resolution coral Ni/Ca data. Further, the WZI involves the only offshore oilfield operations in the coast of Guangxi, with an annual output of approximately 2×10^6 tons of crude oils (Wang et al., 2020). The development of the tourism industry and the prosperity of offshore oilfields have significantly elevated oil spills and oil pollution in the area since 2008. In addition, because the WZI is in the center of the northern Beibu Gulf, which offers access to the sea in the Southwest China, ships likely contribute to the pollution.

Therefore, in the present study, we utilized geochemical proxies (Ni/Ca, $\delta^{18}\text{O}$, $\delta^{13}\text{C}$, etc.) based on a monthly resolution from measurements involving coral skeletons dating back to 1984 in the WZI to evaluate chronological variations of Ni in the surface seawater in the northern SCS. The overall aim of the present study was to reconstruct marine environmental changes in the WZI using the coral Ni/Ca ratio. This investigation enabled an exploration of factors controlling its fluctuations and to evaluate its potential for recording pollution events. The findings of the present study are valuable for assessing the efficiency of environmental law enforcement in local sea areas, marine management of the marine environment, seawater protection, and oil pollution reconstruction.

2. Materials and methods

2.1. Study site

The WZI is a volcanic area in the northern SCS ($109^\circ 05' - 109^\circ 13'E$, $21^\circ 02' - 21^\circ 09'N$), which falls in the south subtropical monsoon climate zone. Annual temperatures in the area range between 15.3°C and 28.9°C , with January as the coldest month and July as the hottest, while the average annual precipitation is ~ 1380.2 mm. The WZI is

unassociated with a perennial river and the marine chemistry is minimally impacted by surrounding continental rivers because of the long distance apart. Weather-related phenomena that significantly impact the WZI include typhoons, rainstorms, cold, and fog. Since exploration started near the WZI in the late 1970s, several oilfields have been discovered and developed. Therefore, crude oil transport and treatment terminals, natural gas plants, and supporting facilities are present in the WZI region (Zhong and Pan, 1997).

Thus, as anthropogenic activities including the development of tourism in the WZI accelerated in recent years, the marine ecological environment was severely impacted, especially because of oil pollution, which has been detected in many places (He et al., 2009). Tourists to the island increased from 9×10^4 in 2005 to 20×10^4 in 2008, while passenger ships correspondingly increased from 1–2 to 4 voyages per day. In 2019, the gross marine revenue of Guangxi increased by 13.4% relative to previous year to 166.4 billion yuan, and this included growth rates of 34.3% and 11.5% for the coastal tourism industry and the marine transportation industry, respectively. The Beihai Port in the south border of Guangxi in the northern SCS connects Guangxi to other areas (Fig. S1).

2.2. Coral sampling

In October 2015, a *Porites* coral was collected from the W3 site ($21^\circ 47'N$, $109^\circ 5'24'E$) in the WZI, northern SCS, at a sampling depth of 4 m (Fig. 1), and was labeled as W3 coral. Near the W3 site, shipping lanes have been operational since 2008. In the laboratory, the colony was cut into slabs measuring ~ 8 cm wide and ~ 1 cm thick along the major growth axis using a cutting machine, followed by drying. Taking the X-ray photos (see Xu et al., 2018), the powder samples were cut intensively along the growth axis of the skeleton slices (with an interval of about 0.5–0.8 mm), and each sample was 15–20 mg.

2.3. Analyses of samples and quality control

In total, 415 powder samples were produced from the coral collected from the W3 site. Approximately 3 mg of coral powder of each sample was placed in a centrifuging tube and ~ 18 g of 2% HNO_3 was added to yield an acid–sample ratio of 6000:1. These samples were used for the determination of major and trace elements. In addition, 3 mg of the coral powder samples were used for measuring the oxygen/carbon isotope ratios of the corals. The $\delta^{18}\text{O}$ and $\delta^{13}\text{C}$ values of the same coral samples have been reported by Xu et al. (2018), and were applied in this study.

The concentrations of Ni and Ca for the samples were determined by inductively coupled plasma mass spectrometry (ICP-MS). In the batch testing process, duplicate samples were utilized for quality control and the testing stability was monitored. Tests were conducted in triplicate and the RSD values were less than 5%. The measurements were performed in the Guangxi laboratory on the Study of Coral Reefs in the South China Sea, Guangxi University. Details on the elemental and isotope measurements were reported in our previous study (Jiang et al., 2020).

2.4. Age model

The annual linear growth (mm/a) of the W3 coral was calculated by measuring the distance between consecutive density couplets along the major axis visible on the X-radiograph. High-resolution $\delta^{18}\text{O}$ data were utilized to validate the growth chronology of the W3 coral by attributing, in which each $\delta^{18}\text{O}$ cycle to 1 year (Xu et al., 2018). Based on the age model and the temperature data from the instrument, and assuming that the consistent growth rates for the corals is consistent, the $\delta^{18}\text{O}$ data were resampled to a monthly resolution through linear interpolation of the summer and winter marker points. The maximum $\delta^{18}\text{O}$ value corresponded to the lowest point of the temperature cycle and vice versa.

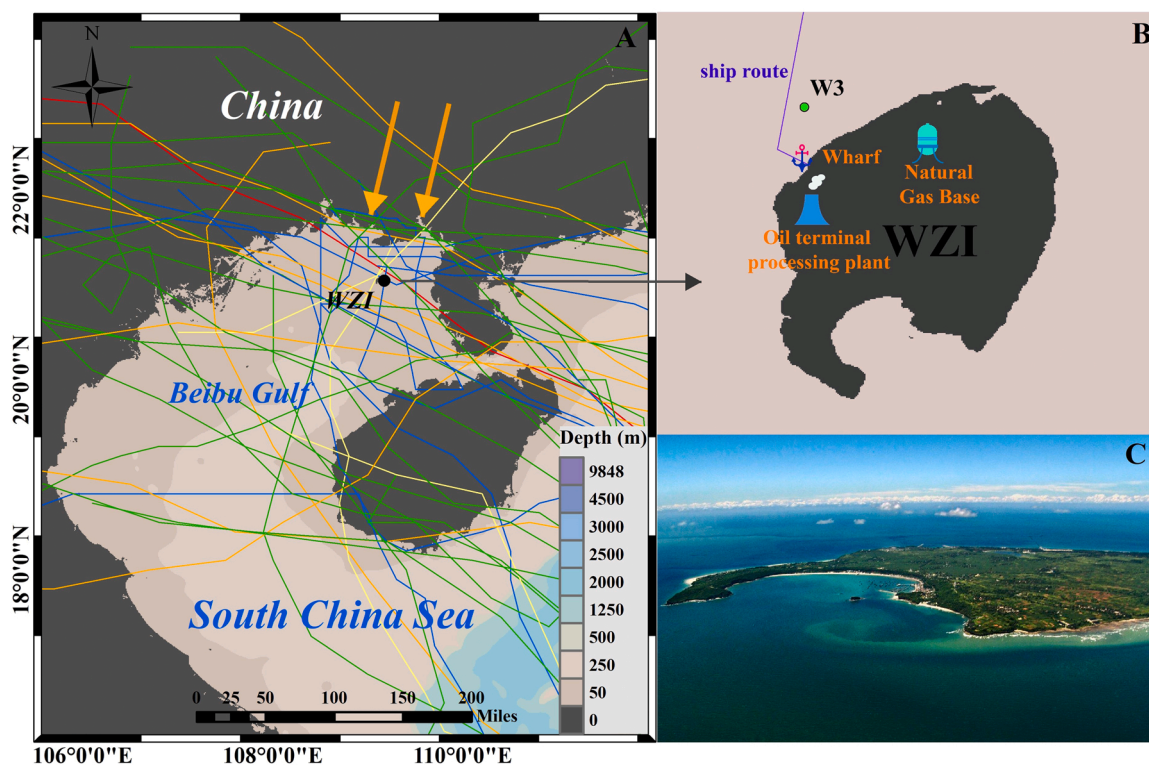


Fig. 1. A) Maps showing the location of the study area (black spot). The colored lines indicate (the colors represent different levels of typhoons near the WZI including the following: red: super typhoon; orange: typhoon; green: severe tropical storm; blue: tropical storm; yellow: tropical depression) represent the typhoon paths identified to affect the WZI during the studied period between 1984 and 2015; B) Illustration of the sampling area showing the location of the W3 coral site (green point) and the wharf (ship's anchor), while the line in purple represents the ship route. Symbols representing the infrastructure near the WZI include the following: blue chimney: oil terminal processing plant; blue oil and gas tank: natural gas base; C) General view of the WZI. Details on the tropical cyclones are provided in Table S1. (For interpretation of the references to color in this figure legend, the reader is referred to the web version of this article.)

However, because of the complex internal structure of corals, the actual growth rates may be inconsistent, and this probably explains the minor deviations in the monthly resolution time series.

2.5. Data processing

The original data in the study were obtained from instrumental determinations, while the monthly resolution data were generated by interpolation of the coral chronology established by assigning the maximum (most positive) and minimum (most negative) $\delta^{18}\text{O}$ values in

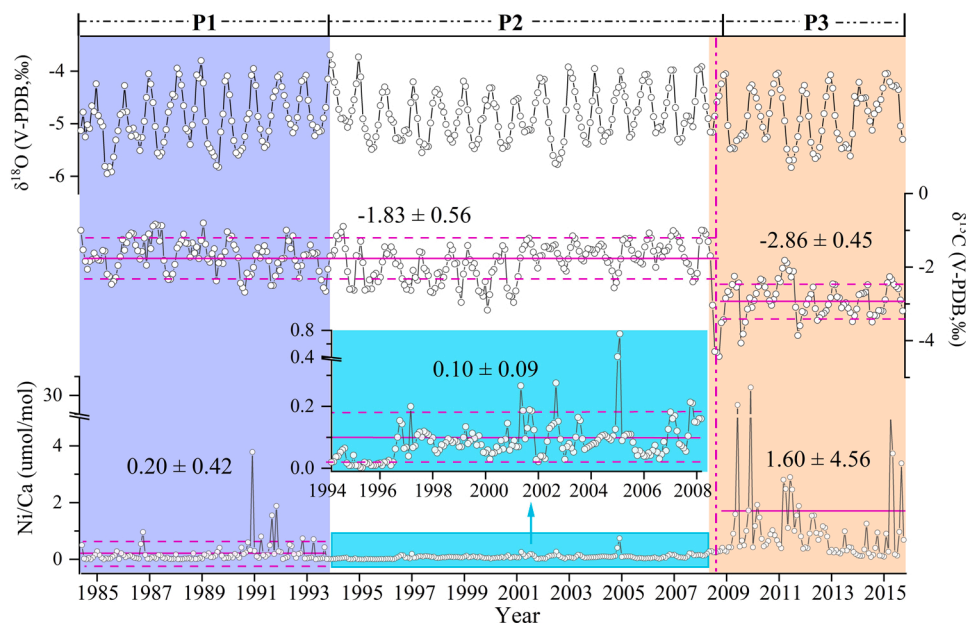


Fig. 2. Plot showing relationships between the Ni/Ca ratios, $\delta^{18}\text{O}$ (V-PDB, ‰), and $\delta^{13}\text{C}$ (V-PDB, ‰) values from the coral skeletons during the period between 1984 and 2015 in the WZI area. This data were interpolated to produce a monthly resolution, thereby yielding 12 points per year. Three periods (P1, P2, and P3) emerged and these are highlighted by distinct colors (purple, white, and orange, respectively). The blue color represents an enlargement showing the coral Ni/Ca ratios during the P2 stage. The coral Ni/Ca ratio data are presented as the mean \pm standard deviation (SD) during each period, and while the coral $\delta^{13}\text{C}$ data are also presented as the mean \pm SD for two stages divided by the broken line in purple. (For interpretation of the references to color in this figure legend, the reader is referred to the web version of this article.)

each annual cycle to the coldest and warmest months of the year, respectively. The annual average coral Ni/Ca data were then obtained from the averages of the interpolated monthly data. Statistical analysis was performed using the SPSS 22.0, while ArcGIS 10.0 was utilized to draw the sampling points map, and Origin 2019 was used to produce charts.

3. Results

Based on the chronologies of the W3 coral (Xu et al., 2018), monthly resolution data representing the period between 1984 and 2015 were obtained. The monthly Ni/Ca ratios from W3 coral vary greatly between 0.0027 and 32.12 $\mu\text{mol/mol}$, with an overall average of $0.46 \pm 2.22 \mu\text{mol/mol}$. As shown in Fig. 2, the coral Ni/Ca data from 1984 to 2015 can be partitioned into three stages. The first stage (P1) involves data from 1984 to 1993, which produced an average of $0.20 \pm 0.42 \mu\text{mol/mol}$, and peaks for most years are significantly smaller than those for 1986 and 1991, which are significantly higher than $0.62 \mu\text{mol/mol}$. The second stage (P2) represents the period from 1994 to 2008, which is characterized by low and stable Ni/Ca ratios, with an average of $0.10 \pm 0.09 \mu\text{mol/mol}$. In the third stage (P3) involving the interval from 2009 to 2015, the Ni/Ca ratios are higher than those for P1 and P2. These exhibit significant fluctuations involving multiple peaks, and ratios range between 0.093 and 32.12 $\mu\text{mol/mol}$, with an average of $1.60 \pm 4.56 \mu\text{mol/mol}$.

The coral Ni/Ca peaks are near points of the negative shift in the coral $\delta^{13}\text{C}$ data, which were previously attributed to oil spills (Xu et al., 2018). In contrast, the coral $\delta^{18}\text{O}$ data essentially stable for the entire study duration (Fig. 2). Considering the background value of Ni in the ocean, the location, and human activities in the study area, we infer that the abnormal Ni peaks in the P1 and P3 stages are associated with anthropogenic activities, while Ni concentrations in the P2 stage are mostly natural.

4. Discussion

4.1. Natural concentration of Ni in surface seawater

The background value of Ni in seawater from around the world varies between 2 and 12 nmol/kg (MBARI, 2012). According to the distribution coefficient of Ni in corals (Saha et al., 2016), we calculated the corresponding seawater Ni during the three periods and compared these to the worldwide average ($\sim 8.2 \text{ nmol/kg}$). The average concentration of Ni in the P2 period is 2.496 nmol/kg, which excluding a few extreme values, reflects the only stage with values that are extreme peaks are within the range for surface seawater worldwide (Fig. 3). Thus, we used this period to highlight natural characteristics of Ni in surface seawater.

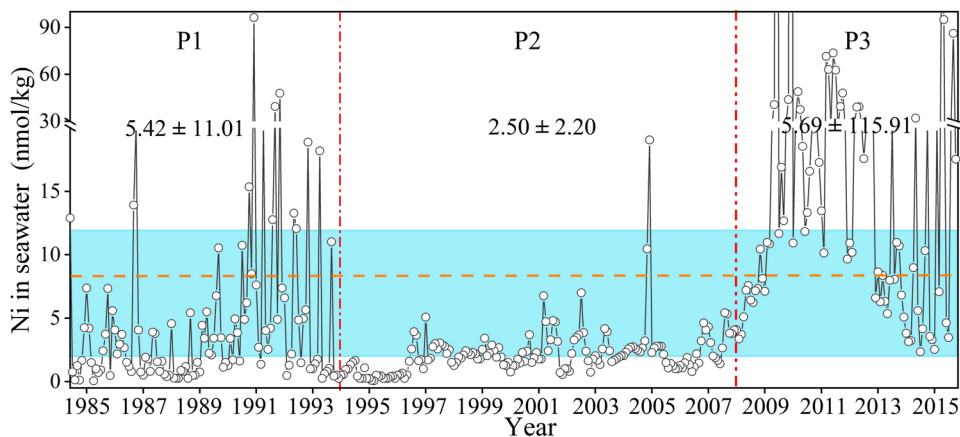


Fig. 3. Plot showing Ni concentration in W3 coral after conversion to the concentration range in seawater (the area in blue represents the background concentrations of Ni in ocean worldwide (2–12 nmol/kg), while the broken line in orange represents the global average concentration (8.2 nmol/kg)). The seawater Ni concentrations are presented as the mean \pm SD for three stages divided by the broken line in red. (For interpretation of the references to color in this figure legend, the reader is referred to the web version of this article.)

River input is a significant source of the dissolved Ni in the ocean, and this load represents a substantial portion of the total loads (Revels et al., 2021). In addition, runoff associated with heavy rainfall transports significant terrigenous materials into coastal waters. Owing to the strong adsorption capacity of sediments for heavy metals, transported Ni is quickly adsorbed to form stable complexes with sediments (Liang et al., 2005). In the northern SCS, heavy rainfall is restricted to the wet season (April–September), and as shown in Fig. S2, the coral Ni/Ca ratios exhibit obvious seasonal variations. To confirm the relationship between the Ni concentrations and rainfall, we compared data for the wet and dry seasons. In the P2 stage, the coral Ni/Ca values for most years, especially before 2004, are higher in the wet than in the dry season (Fig. 4). To test the strength and stationarity of the relationship between local precipitation and the monthly Ni/Ca ratios from 1994 to 2008 and to eliminate effects of deviations in the interpolation time series, the sliding-window correlation analysis was performed using a 12-month moving window. Fig. S3 shows that precipitation and the coral Ni/Ca ratios are significantly correlated because most sliding correlation coefficients are > 0.3 ($p < 0.01$). However, according to previous studies on the wet deposition flux studies, rainwater minimally contributes to the total Ni deposition (Chance et al., 2015; Wang et al., 2017). Further, the site of the coral studied is quite far from the mainland and owing to the absence of perennial rivers in the WZI, the contribution of Ni from riverine sources to the surface seawater is likely negligible.

Therefore, high Ni in the summer during the P2 period is associated with another source linked to high precipitation. The WZI falls in the monsoon climate zone, which is mainly characterized by the monsoon and tropical cyclones during intense precipitation in the summer (Zhang et al., 2017). In addition to rainfall, these weather-related phenomena are often accompanied by strong winds (Zhang et al., 2017), and thus, the impact of such winds requires consideration. Ni is a biologically active element that exhibits characteristics of nutrients in modern oceans (Sutherland and Costa, 2002; Aciego et al., 2015). Continental shelf sediments represent an important source of dissolved trace metals in the ocean, and river-transported sediments are abundant in the SCS shelf area (Lalraj and Nair, 2006; Liu et al., 2016). Strong winds can weaken the seawater stratification and alter redox conditions in water overlying the marine sediments. Under such circumstances, Ni in the relatively enriched bottom water migrates to the surface, and coupling of this the reactivation and mixing enhances dissolved Ni in the surface water (Guan et al., 2021). The wind speeds, coral Ni/Ca ratios, and rainfall in Fig. 5, reveals an average coral Ni/Ca ratio of 0.11 $\mu\text{mol/mol}$ in the summer, which is significantly higher than the winter average of 0.07 $\mu\text{mol/mol}$. Therefore, the remobilization of Ni in marine sediments and the subsequent transport to the surface seawater because of vertical mixing triggered by winds may contribute to elevating the surface seawater Ni concentrations.

The annual average coral Ni/Ca ratios and the East Asian summer

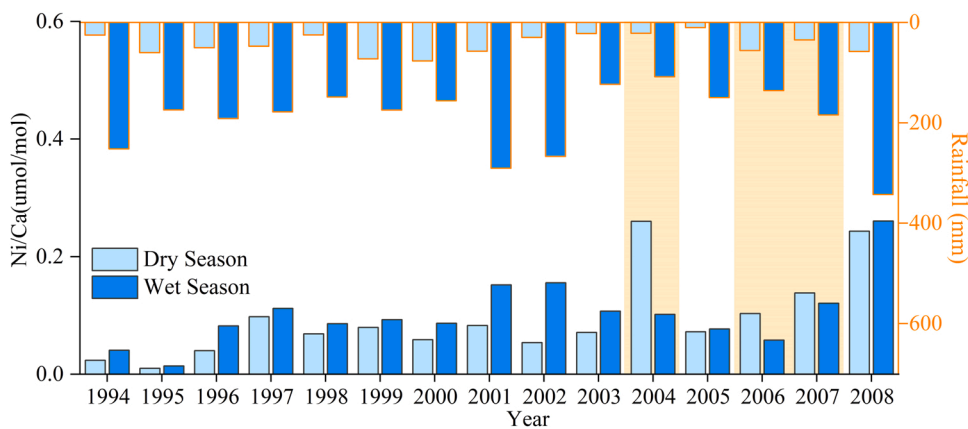


Fig. 4. Time series highlighting annual changes in geochemical indicators for the W3 coral in the WZI (1994–2008) and precipitation in the dry and wet seasons. The black border light blue and dark blue histograms represent the annual averages of Ni/Ca in the dry and wet seasons, respectively, while the orange border light blue and dark blue histograms display the annual average rainfall in the dry season and wet seasons, respectively. The orange background indicates a period characterized by inconsistent trends. (For interpretation of the references to color in this figure legend, the reader is referred to the web version of this article.)

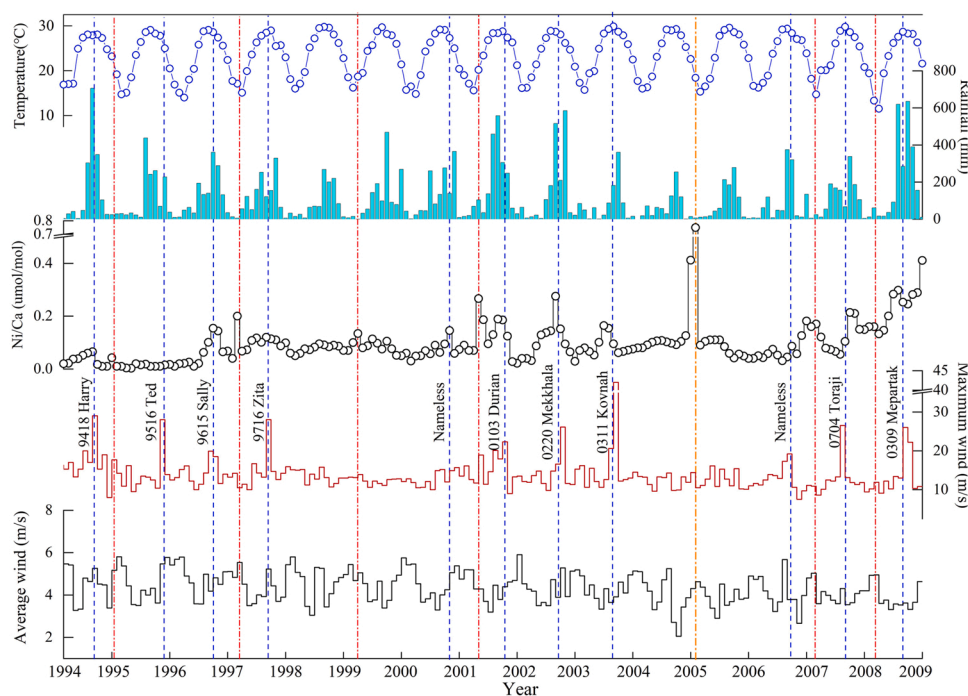


Fig. 5. Plots showing relationships between the coral Ni/Ca ratios, average wind speed, maximum wind speed, rainfall and temperature in the WZI between 1994 and 2009. The dotted lines represent abrupt peaks in the coral Ni/Ca data, while blue dotted lines indicate abrupt peaks in the coral Ni/Ca data which are probably linked to tropical cyclones (codes and names of typhoons are provided near the lines), and the red chain lines in the winter depict abrupt coral Ni/Ca ratio peaks probably related to the winter monsoon. The orange chain line represents abrupt peaks in the coral Ni/Ca data probably related to artificial disturbances (wind speed data from the global greenhouse data system). (For interpretation of the references to color in this figure legend, the reader is referred to the web version of this article.)

monsoon index (Li and Zeng, 2005) exhibit no correlation (Fig. S4). Therefore, monsoon-derived Ni cannot explain temporal changes in the surface seawater Ni concentrations. However, the strong correlation between the coral Ni/Ca ratios and the maximum wind speeds in the WZI shown in Figs. 5 and S5 highlights possible effects of tropical cyclones and winter monsoons on the WZI. This suggests that the weakening of the seawater stratification and alteration of redox conditions in the bottom water attributed to strong winds along with tropical cyclones are responsible for the seasonal variations in the surface seawater Ni concentrations. Nevertheless, the coral Ni/Ca data in Fig. 5 involve abrupt variations in the winter which cannot be explained by the tropical cyclones. Therefore, the strong winter monsoon is the dominant driver that diminished seawater Ni stratification in the Beibu Gulf (Tang et al., 2003), and thus, increased the surface seawater Ni concentrations, similar to the concentrations of REEs and V reported by Li et al. (2019) and Steven and Sarah (1991), respectively.

4.2. Reliability of coral Ni/Ca as a proxy of oil pollution

The increase in Ni concentrations in oceans is closely related to

anthropogenic sources, such as the shipping industry and oil field exploitation (Li and Schoonmaker, 2003; Liu et al., 2015). The dissolution of oil, for example, can release abundant Ni to the water column (Santos-Echeandía et al., 2005). Li et al. (2015) and Xu et al. (2019) reported pollution of sediments in many areas of the Beibu Gulf, and the pollution was primarily attributed to petroleum. Pollution by petroleum can be associated with the drilling of oil, sewage discharge, and oil transportation (Liu et al., 2015). Therefore, because of the continuous development of offshore oil and gas platforms as well as the marine transportation industry in the WZI, oil pollution has been increasing (Chen, 2014; Chen et al., 2018). Based on the history of the development of oilfields and the incidence of oil spills in the WZI (Zhong and Pan, 1997), we observed that the coral Ni/Ca ratio fluctuations are closely linked to oil pollution (Figs. 6 and 7).

Evidently, the high coral Ni/Ca ratios in 1986 and 1991 coincide with the production periods of the WZ10-3 and WZ11-4 oilfields in the P1 stage. During the oilfield development stage, the Ni/Ca ratio fluctuates significantly, and then relatively stabilizes after production began. In the initial stage of the development of an oilfield, pollutants can be dispersed in the surrounding environment, and the subsequent

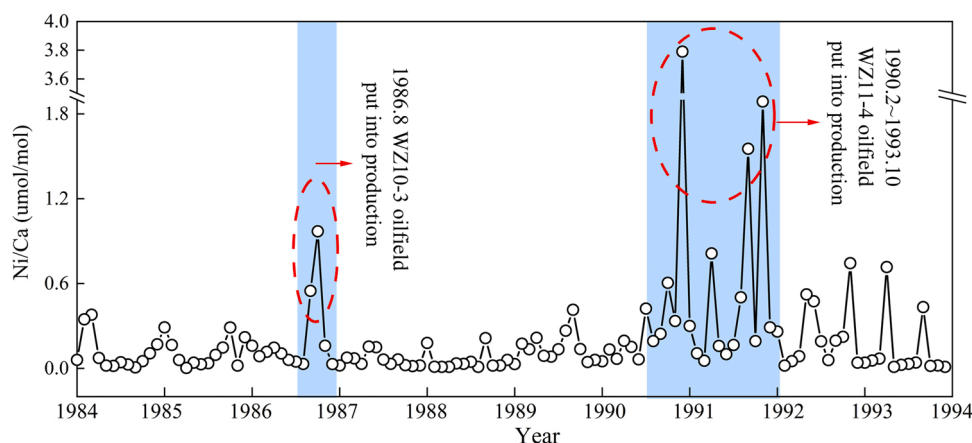


Fig. 6. Time series of the Ni/Ca ratios from W3 coral skeletons (1984–1993). The Ni/Ca ratios in the blue background and red circle corresponded to the development and production periods of the WZ10-3 and WZ11-4 oilfields. (For interpretation of the references to color in this figure legend, the reader is referred to the web version of this article.)

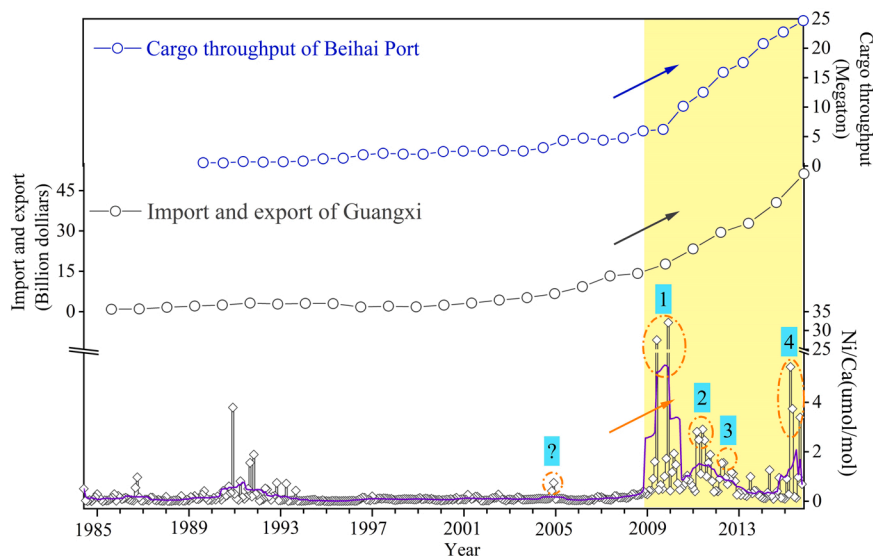


Fig. 7. Plot showing relationships between the W3 coral Ni/Ca ratios, the import and export in Guangxi, and the cargo throughput in the Beihai Port between 1985 and 2015. The bolded lines represent 3-year (36 months) running averages, while arrows indicates an abrupt increase or decline. The area in yellow represents the P3 period, and the four orange circles show that the coral Ni/Ca ratios higher than the average are coincide with four oil spill incidents, while the circled question mark indicates possible artificial disturbances. (For interpretation of the references to color in this figure legend, the reader is referred to the web version of this article.)

Data sources: Guangxi Statistical Yearbook (Guangxi Zhuang Autonomous Region Statistics Bureau, 2016).

entry of such pollutants into seawater (Chen, 2014; Jurado et al., 2005; Lucey et al., 2001) can explain the abrupt variations in the coral Ni/Ca ratios observed in the study area. Meanwhile, because oil production involves controllable discharges, the associated pollution is reduced (Shamkhani, 2013). These results demonstrate that the coral Ni/Ca ratios of the colony from the W3 site adequately reflect the oilfield development history in the WZI.

Beyond 2008, the coral Ni/Ca ratio plot involves multiple abrupt peaks (Fig. 2), which coincided with reported oil spills in 2009, 2011, 2012, and 2014 in the WZI area (Fig. 7). The highest values (27.5–32.1 $\mu\text{mol/mol}$) appear in 2009, when oil measuring ~ 500 m in length and ~ 10 m in width of drifted through wave activity from an oilfield and appeared offshore in the west of the WZI. Several peaks are present in the coral Ni/Ca ratio (2.4–2.9 $\mu\text{mol/mol}$) plot for 2011, when ~ 3 km² floating oil emerged in the west coast of the WZI. Minor peaks (~ 1.55 $\mu\text{mol/mol}$) are also observed in 2012 when approximately 10 tons of diesel oil leaked from a damaged ship. Prominent peaks (3.4–5.4 $\mu\text{mol/mol}$) abruptly appear in 2014 because of several tons of bunker oils that leaked after a cargo ship accident in the west wharf of the WZI. The plot of $\delta^{13}\text{C}$ values of W3 coral reported by Xu et al. (2018) exhibited many abrupt negative shifts after ~ 2008 , and these were also attributed to oil spills. Considering the deviation of the age model

(Gagan et al., 2012), the coral Ni/Ca ratios adequately recorded four oil spills in the WZI area, and these results confirm that it is a reliable proxy for oil pollution in the marine environment. Therefore, the abrupt elevated coral Ni/Ca ratios in 2004 may be associated with an unknown oil spill (Fig. 7), and this probably explains the elevated ratios during the dry season in 2004 (Fig. 4).

4.3. Industrial transformation in the SCS area based on seawater Ni

Deforestation, agriculture, mining and metallurgical industry activities as well as coal and oil usage alter the biogeochemical cycles of many trace elements (Sen and Peucker-Ehrenbrink, 2012). After deposition on marine sediments as non-volatile components of crude oils, metals such as Ni may be adsorbed, thereby elevating its concentration in the continental shelf (Steffy et al., 2013). In the present study, Ni concentrations data of W3 coral in the WZI were used to reconstruct variations of Ni concentration in the surface seawater. These data are further examined to assess their relationship to industrial transformation in the area. Around 1992, a significant decline is observed in the plot of the coral Ni/Ca ratios (Fig. 7), and this is probably associated with environmental protection measures in the Environmental Protection Law introduced in the People's Republic of China at the end of

1989.

The SCS receives abundant sediments from nearby rivers (Liu et al., 2016), and thus, dissolved trace metals can be easily transported to the WZI on the continental shelf (Li et al., 2019; Rea and Ruff, 1996). According to Ho et al. (2011) and Takano et al. (2020), winds and rivers exert varying influences on the stratification of Ni in the northern SCS. Possibly, the anthropogenic Ni input from fluvial sediments in the Beibu Gulf before 1992 concealed the impacts of winds (Zhao et al., 1995). However, after 1992, winds were supposed to dominantly control the surface seawater Ni concentrations because of the decline in anthropogenic Ni inputs related to the environmental protection measures. Despite the minor contribution of dissolved Ni from rivers to the surface seawater in the WZI area, the impact of Ni transported to the continental shelf from marine sediments cannot be neglected. Notably, this transportation of Ni from estuaries to the continental shelf is a slow process (Wang et al., 2018). This supports the decline in anthropogenic Ni contribution in the early 1990s after the introduction of Environmental Protection Law in China.

The relatively low Ni concentrations lasted ~ 14 years, and then increased suddenly in 2009. Ships became the principal sources of pollutants in the WZI, as the development of tourism and offshore oilfields proceeded (Gao et al., 2017). Tao et al. (2017) and Zhao et al. (2021) reported that ship transportation was an important source of Ni contribution in coastal regions, including the northern SCS. Ni emissions to the atmosphere can affect the surface seawater near the source vessels through deposition and dissolution (Endres et al., 2018), and these can be recorded in coral skeletons. As shown in Fig. 7, the import and export volume in Guangxi have significantly increased since 2009. In fact, the import and export volume in Guangxi and the throughput of Beihai Port both suddenly changed around 2008, and continued to grow significantly growth (Fig. 7). Considering that the W3 site is near the busiest sea route in the study area, we infer that local pollution sources associated with the development of the shipping industry dominantly account for the increase in Ni contributions during the P3 stage, and this was independent of the elevated Ni contributions in the P1 stage. Clearly, the coral inferred Ni contributions in the WZI area mainly depended on the revolution and development of the industry in the Beibu Gulf. Coincidentally, because of changes in fuel usage and industrial practices, a similar trend emerged in Ni contributions in some areas in the past decades. That is, reduction because of environmental protection policies and increase caused by transportation and industrial development (Allan et al., 2013; Marx et al., 2010; Pontevedra-Pombal et al., 2013).

In summary, anthropogenic contributions of Ni in the northern SCS reveal the following stages of industrial change: 1) a high-contribution stage dominated by traditional industrial and agricultural activities; 2) a sustained low-contribution stage that was promoted by environmental protection measures; 3) a booming stage involving the development of the transportation industry, especially the shipping industry, which involved several unusual peaks related to oil spills.

5. Conclusion

In the present study, Ni/Ca ratios were determined using coral skeletons collected from the WZI in the central part of the Beibu Gulf, and monthly Ni concentrations in the surface seawater from 1984 to 2015 were estimated. The temporal evolution of the Ni concentrations revealed industrial transformation in the Beibu Gulf. During the 32 years involved in the present study, significant increases in the concentrations of Ni in surface seawater in the study area were directly related to human activities. The P1 stage was characterized by relatively high coral Ni/Ca ratios, which indicated contributions from industrial and agricultural activities in the surrounding areas, such as, exploration, production, and transportation in oilfields near the WZI. In the P2 stage, the coral Ni/Ca ratios significantly declined because of the implementation of the Environmental Protection Law introduced at the end of 1989 CE.

Conversely, in the P3 stage, the coral Ni/Ca ratios were the highest because offshore the operations linked to the development and operation of the Beibu Gulf Economic Zone from 2009, which were associated with several oil spills. Besides human activities, Ni concentrations also highlighted the impact of surface winds linked to tropical cyclones in the summer and monsoons in the winter in the study area. Considering the rapid development of offshore oilfields and marine transportation, the coral Ni/Ca ratio exhibited potential for reconstructing the oil pollution history. The findings of the present study are valuable for testing the efficiency of environmental law enforcement in local sea areas and this can be applied in other areas affected by oil pollution where corals are present around the world.

CRediT authorship contribution statement

Xingyuan Wu: Investigation, Methodology, Formal analysis, Writing – original draft. **Wei Jiang:** Conceptualization, Methodology, Formal analysis, Writing – review & editing, Resources. **Kefu Yu:** Conceptualization, Data curation, Writing – review & editing, Funding acquisition, Resources, Supervision. **Shendong Xu:** Methodology, Data curation, Writing – review & editing. **Haodan Yang:** Investigation, Methodology, Writing – review & editing. **Ning Wang:** Investigation, Data curation. **Chaoshuai Wei:** Methodology, Data curation. **Chunmei Feng:** Investigation, Methodology. **Yinan Sun:** Investigation, Methodology. **Sirong Xie:** Investigation, Methodology.

Declaration of Competing Interest

The authors declare that they have no known competing financial interests or personal relationships that could have appeared to influence the work reported in this paper.

Acknowledgments

This research was supported by the National Natural Science Foundation of China (Grant Nos. 42030502, 41976059, and 42090041), the Guangxi Scientific Projects (Grant Nos. 2019GXNSFAA185022, AD17129063, and AA17204074) and the project supported by Innovation Group Project of Southern Marine Science and Engineering Guangdong Laboratory (Zhuhai) (No. 311019006/311020006). The data used in this paper will be deposited in a general data repository (<https://doi.org/10.6084/m9.figshare.16756270.v1>). Thanks are due to the responsible editor and four anonymous reviewers for their critical reviews and constructive comments, which helped us improve our paper significantly.

Attestations

We have uploaded our manuscript “Coral-inferred historical changes of nickel emissions related to industrial and transportation activities in the Beibu Gulf, northern South China Sea”, by Xingyuan Wu, Wei Jiang, Kefu Yu, Shendong Xu, Haodan Yang, Ning Wang, Chaoshuai Wei, Chunmei Feng, Yinan Sun, Sirong Xie. We would like it to be considered for publication in Journal of Hazardous Materials.

Authorship

No conflict of interest exists in the submission of this manuscript, and the manuscript is approved by all authors for publication.

Prior publication

The work described was original research that has not been published previously and not under consideration for publication elsewhere, in whole or in part.

Art

All photos and images were generated by authors and comply with the requirements listed in the Author Guidelines.

Appendix A. Supplementary material

Supplementary data associated with this article can be found in the online version at [doi:10.1016/j.jhazmat.2021.127422](https://doi.org/10.1016/j.jhazmat.2021.127422).

References

- Aciego, S.M., Stevenson, E.I., Arendt, C.A., 2015. Climate versus geological controls on glacial meltwater micronutrient production in Southern Greenland. *Earth Planet. Sci. Lett.* 424, 51–58. <https://doi.org/10.1016/j.epsl.2015.05.017>.
- Alharbi, T., Alfaihi, H., El-Sorogy, A., 2017. Metal pollution in Al-Khobar seawater, Arabian Gulf, Saudi Arabia. *Mar. Pollut. Bull.* 119 (1), 407–415. <https://doi.org/10.1016/j.marpolbul.2017.03.011>.
- Ali, A., Hamed, M.A., El-Azim, H.A., 2011. Heavy metals distribution in the coral reef ecosystems of the Northern Red Sea. *Helgol. Mar. Res.* 65 (1), 67–80. <https://doi.org/10.1007/s10152-010-0202-7>.
- Allan, M., Le Roux, G., De Vleeschouwer, F., Bindler, R., Blaauw, M., Piotrowska, N., Sikorski, J., Fagel, N., 2013. High-resolution reconstruction of atmospheric deposition of trace metals and metalloids since AD 1400 recorded by ombrotrophic peat cores in Hautes-Fagnes, Belgium. *Environ. Pollut.* 178, 381–394. <https://doi.org/10.1016/j.envpol.2013.03.018>.
- Amorosi, A., 2012. Chromium and nickel as indicators of source-to-sink sediment transfer in a Holocene alluvial and coastal system (Po Plain, Italy). *Sediment. Geol.* 280, 260–269. <https://doi.org/10.1016/j.sedgeo.2012.04.011>.
- Archer, C., Vance, D., Milne, A., Lohan, M., 2020. The oceanic biogeochemistry of nickel and its isotopes: new data from the South Atlantic and the Southern Ocean biogeochemical divide. *Earth Planet. Sci. Lett.* 535, 116118. <https://doi.org/10.1016/j.epsl.2020.116118>.
- Bastidas, C., Garcia, E., 1999. Metal content on the reef coral porites astreoides: an evaluation of river influence and 35 years of chronology. *Mar. Pollut. Bull.* 38 (10), 899–907. [https://doi.org/10.1016/S0025-326X\(99\)00089-2](https://doi.org/10.1016/S0025-326X(99)00089-2).
- Cantú, R., Stencil, J.R., Czernuszewicz, R.S., Jaffé, P.R., Lash, T.D., 2000. Surfactant-enhanced partitioning of nickel and vanadyl deoxyphloerythroiochlorophylls from crude oil into water and their analysis using surface-enhanced resonance Raman spectroscopy. *Environ. Sci. Technol.* 34 (1), 192–198. <https://doi.org/10.1021/es990213s>.
- Celo, V., Dabek-Zlotorzynska, E., McCurdy, M., 2015. Chemical characterization of exhaust emissions from selected Canadian marine vessels: the case of trace metals and lanthanoids. *Environ. Sci. Technol.* 49, 5220–5226. <https://doi.org/10.1021/acs.est.5b00127>.
- Chance, R., Jickells, T.D., Baker, A.R., 2015. Atmospheric trace metal concentrations, solubility and deposition fluxes in remote marine air over the south-east Atlantic. *Mar. Chem.* 177, 45–56. <https://doi.org/10.1016/j.marchem.2015.06.028>.
- Chen, J., Zhang, W., Li, S., Zhang, F., Zhu, Y., Huang, X., 2018. Identifying critical factors of oil spill in the tanker shipping industry worldwide. *J. Clean. Prod.* 180, 1–10. <https://doi.org/10.1016/j.jclepro.2017.12.238>.
- Chen, Y., 2014. *Impact of Marine Oil Pollution and Emergency Management in Beibu Gulf of Guangxi*. Ocean University of China, Qingdao, China.
- Corbin, J.C., Mensah, A.A., Pieber, S.M., Orasche, J., Michalke, B., Zanatta, M., Czech, H., Massabò, D., Buatier de Mongeot, F., Mennucci, C., El Haddad, I., Kumar, N.K., Stengel, B., Huang, Y., Zimmermann, R., Prévôt, A.S.H., Gysel, M., 2018. Trace metals in soot and PM_{2.5} from heavy-fuel-oil combustion in a marine engine. *Environ. Sci. Technol.* 52, 6714–6722. <https://doi.org/10.1021/acs.est.8b01764>.
- Dechaine, G.P., Gray, M.R., 2010. Chemistry and association of vanadium compounds in heavy oil and bitumen, and implications for their selective removal. *Energy Fuels* 24, 2795–2808. <https://doi.org/10.1021/ef100173j>.
- Dupont, C.L., Buck, K.N., Palenik, B., Barbeau, K., 2009. Nickel utilization in phytoplankton assemblages from contrasting oceanic regimes. *Deep Sea Res. Part I Oceanogr. Res. Pap.* 57 (4), 553–566. <https://doi.org/10.1016/j.dsr.2009.12.014>.
- Endres, S., Maes, F., Hopkins, F., Houghton, K., Mårtensson, E.M., Oeffner, J., Quack, B., Singh, P., Turner, D., 2018. A new perspective at the ship-air-sea-interface: the environmental impacts of exhaust gas scrubber discharge. *Front. Mar. Sci.* 5, 139. <https://doi.org/10.3389/fmars.2018.00139>.
- Gagan, M.K., Ayliffe, L.K., Beck, J.W., Cole, J.E., Druffel, E.R.M., Dunbar, R.B., Schrag, D.P., 2000. New views of tropical paleoclimates from corals. *Quat. Sci. Rev.* 19, 45–64.
- Gagan, M.K., Dunbar, G.B., Suzuki, A., 2012. The effect of skeletal mass accumulation in Porites on coral Sr/Ca and $\delta^{18}O$ paleothermometry. *Paleoceanography* 27 (1), n/a. <https://doi.org/10.1029/2011PA002215>.
- Gaillardet, J., Viers, J., Dupré, B., 2003. Trace elements in river waters. *Treatise on Geochemistry. Surface and Ground Water, Weathering, and Soils*, 5, pp. 225–272. <https://doi.org/10.1016/B0-08-043751-6/05165-3>.
- Gao, Y.G., Zhang, K., Wang, T.J., Chen, Z.M., Geng, H., Meng, F., 2017. Concentration characteristics and influencing factors of atmospheric particulate matters in spring on Weizhou Island, Beihai, Guangxi Province. *Environ. Sci.* 38, 1753–1759. <https://doi.org/10.13227/j.hjkk.201609104>.
- Gillmore, M.L., Gissi, F., Golding, L.A., Stauber, J.L., Reichelt-Brushett, A.J., Severati, A., Humphrey, C.A., Jolley, D.F., 2020. Effects of dissolved nickel and nickel-contaminated suspended sediment on the scleractinian coral, *Acropora muricata*. *Mar. Pollut. Bull.* 152, 110886. <https://doi.org/10.1016/j.marpolbul.2020.110886>.
- Gissi, F., Reichelt-Brushett, A.J., Chariton, A.A., Stauber, J.L., Greenfield, P., Humphrey, C., Salmon, M., Stephenson, S.A., Cresswell, T., Jolley, D.F., 2019. The effect of dissolved nickel and copper on the adult coral *Acropora muricata* and its microbiome. *Environ. Pollut.* 250, 792–806. <https://doi.org/10.1016/j.envpol.2019.04.030>.
- Guan, S., Zhao, W., Sun, L., Zhou, C., Liu, Z., Hong, X., Zhang, Y., Tian, J., Hou, Y., 2021. Tropical cyclone-induced sea surface cooling over the Yellow Sea and Bohai Sea in the 2019 Pacific typhoon season. *J. Mar. Syst.* 217, 103509. <https://doi.org/10.1016/j.jmarsys.2021.103509>.
- Guangxi Zhuang Autonomous Region Statistics Bureau, 2016. *Guangxi Statistical Yearbook-2016*. China Statistics Press. (<http://tjj.gxzf.gov.cn/tjsj/tjnj/>).
- Guzmán, H.M., Jarvis, E.J., 1992. Contamination of coral reefs by heavy metals along the Caribbean coast of Central America (Costa Rica and Panama). *Mar. Pollut. Bull.* 24, 554–561. [https://doi.org/10.1016/0025-326X\(92\)90708-E](https://doi.org/10.1016/0025-326X(92)90708-E).
- Guzmán, H.M., Jarvis, K.E., 1996. Vanadium century record from caribbean reef corals: a tracer of oil pollution in Panama. *Ambio* 25 (8), 523–523.
- He, G., Yuan, G., Lin, D., Cai, W., Lei, F., 2009. Influence of oil-field exploitation on marine environment: a case study of Wei-zhou on-feld. *Mar. Environ. Sci.* 28 (2), 198–201.
- Ho, T., Chou, W., Lin, H., Sheu, D., 2011. Trace metal cycling in the deep water of the South China Sea: the composition, sources, and fluxes of sinking particles. *Limnol. Oceanogr.* 56 (4), 1225–1243. <https://doi.org/10.4319/lo.2011.56.4.1225>.
- Jayaraju, N., Sundara Raja Reddy, B.C., Reddy, K.R., 2009. Heavy metal pollution in reef corals of Tuticorin Coast, Southeast Coast of India. *Soil Sediment Contam.* 18, 445–454. <https://doi.org/10.1080/15320380902962361>.
- Jiang, W., Yu, K., Wang, N., Yang, H., Yang, H., Xu, S., Wei, C., Wang, S., Wang, Y., 2020. Distribution coefficients of trace metals between coral lattices and seawater in the northern South China Sea: species and SST dependencies. *J. Asian Earth Sci.* 187, 104082.1–104082.8. <https://doi.org/10.1016/j.jseas.2019.104082>.
- Jurado, E., Jaward, F., Lohmann, R., Jones, K., Simo, R., Dachs, J., 2005. Wet deposition of persistent organic pollutants to the global oceans. *Environ. Sci. Technol.* 39 (8), 2426–2435. <https://doi.org/10.1021/es048599g>.
- Kadko, D., Aguilar-Islas, A., Bolt, C., Buck, C.S., Fitzsimmons, J.N., Jensen, L.T., Landing, W.M., Marsay, C.M., Rember, R., Shiller, A.M., Whitmore, L.M., Anderson, R.F., 2019. The residence times of trace elements determined in the surface Arctic Ocean during the 2015 US Arctic geotraces expedition. *Mar. Chem.* 208 (20), 56–69. <https://doi.org/10.1016/j.marchem.2018.10.011>.
- Lalura, C.M., Nair, S.M., 2006. Geochemical index of trace metals in the surficial sediments from the western continental shelf of India, Arabian sea. *Environ. Geochem. Health* 28 (6), 509–518. <https://doi.org/10.1007/s10653-005-8619-7>.
- Li, J.P., Zeng, Q.C., 2005. A new monsoon index, its interannual variability and relation with monsoon precipitation. *Clim. Environ. Res.* 351–365. <https://doi.org/10.3878/j.issn.1006-9585.2005.03.09>.
- Li, P., Rui, X., Wang, Y., Zhang, R., Zhang, G., 2015. Influence of anthropogenic activities on paxs in sediments in a significant gulf of low-latitude developing regions, the Beibu Gulf, South China Sea: distribution, sources, inventory and probability risk. *Mar. Pollut. Bull.* 90 (1–2), 218–226. <https://doi.org/10.1016/j.marpolbul.2014.10.048>.
- Li, X., Liu, Y., Wu, C.C., Sun, R., Zheng, L., Lone, M.A., Shen, C.C., 2019. Coral-inferred monsoon and biologically driven fractionation of offshore seawater rare earth elements in Beibu Gulf, northern South China Sea. *Solid Earth Sci.* 4, 131–141. <https://doi.org/10.1016/j.sesci.2019.09.003>.
- Li, Y.H., Schoonmaker, J.E., 2003. Chemical composition and mineralogy of marine sediments. *Treatise Geochem.* 7, 1–35. <https://doi.org/10.1016/B0-08-043751-6/07088-2>.
- Liang, W.J., Li, J., Zhao, C.L., Fan, L.D., Jin C., Y., 2005. Release of heavy metals Ni and Zn in sediments of Taiyuan Section of Fenhe River. *J. Beijing Univ. Technol.* 02, 174–178. <https://doi.org/10.3969/j.issn.0254-0037.2005.02.014>.
- Liu, X., Meng, R., Xing, Q., Lou, M., Chao, H., Bing, L., 2015. Assessing oil spill risk in the Chinese Bohai Sea: a case study for both ship and platform related oil spills. *Ocean Coast. Manag.* 108, 140–146. <https://doi.org/10.1016/j.ocecoaman.2014.08.016>.
- Liu, Z., Zhao, Y., Colin, C., Statterger, K., Wiesner, M.G., Huh, C.-A., Zhang, Y., Li, X., Sompongchaiyakul, P., You, C.F., Huang, C.Y., Liu, J.T., Siringan, F.P., Le, K.P., Sathiamurthy, E., Hantoro, W.S., Liu, J., Tuo, S., Zhao, S., Zhou, S., He, Z., Wang, Y., Bunsomboonsakul, S., Li, Y., 2016. Source-to-sink transport processes of fluvial sediments in the South China Sea. *Earth-Sci. Rev.* 153, 238–273. <https://doi.org/10.1016/j.earscirev.2015.08.005>.
- López, L., Lo Mónaco, S., 2017. Vanadium, nickel and sulfur in crude oils and source rocks and their relationship with biomarkers: implications for the origin of crude oils in Venezuelan basins. *Org. Geochem.* 104, 53–68. <https://doi.org/10.1016/j.orggeochem.2016.11.007>.
- Lough, J.M., 2010. Climate records from corals. *Wiley Interdiscip. Rev. Clim. Chang.* 1. <https://doi.org/10.1002/wcc.39>.
- Lucey, D., Hadjiiski, L., Hopke, P.K., Scudlark, J.R., Church, T., 2001. Identification of sources of pollutants in precipitation measured at the mid-Atlantic US coast using potential source contribution function (PSCF). *Atmos. Environ.* 35, 3979–3986. [https://doi.org/10.1016/S1352-2310\(01\)00185-6](https://doi.org/10.1016/S1352-2310(01)00185-6).
- Mackey, D., O'Sullivan, J., Watson, R., Dal Pont, G., 2002. Trace metals in the Western Pacific: temporal and spatial variability in the concentrations of Cd, Cu, Mn and Ni. *Deep Sea Res. Part I Oceanogr. Res. Pap.* 49, 2241–2259. [https://doi.org/10.1016/S0967-0637\(02\)00124-3](https://doi.org/10.1016/S0967-0637(02)00124-3).

- Marx, S.K., Kamber, B.S., McGowan, H.A., Zawadzki, A., 2010. Atmospheric pollutants in alpine peat bogs record a detailed chronology of industrial and agricultural development on the Australian continent. *Environ. Pollut.* 158, 1615–1628. <https://doi.org/10.1016/j.envpol.2009.12.009>.
- MBARI, 2012. The Monterey Bay Aquarium Research Institute Chemical Sensor Program: Periodic Table of Elements in the Ocean. (<http://www.mbari.org/chemsensor/pteo.htm>).
- Mokhtar, M.B., Praveena, S.M., Aris, A.Z., Yong, O.C., Lim, A.P., 2012. Trace metal (Cd, Cu, Fe, Mn, Ni and Zn) accumulation in Scleractinian corals: a record for Sabah, Borneo. *Mar. Pollut. Bull.* 64, 2556–2563. <https://doi.org/10.1016/j.marpolbul.2012.07.030>.
- Nicolas, D., Patrick, D.D., Stephen, E., Stewart, F., Claude, P., 2018. A record of mining and industrial activities in New Caledonia based on trace elements in rhodolith-forming coralline red algae. *Chem. Geol.* 493, 24–36. <https://doi.org/10.1016/j.chemgeo.2018.05.014>.
- Pontevedra-Pombal, X., Mighall, T.M., Nóvoa-Muñoz, J.C., Peiteado-Varela, E., Rodríguez-Racedo, J., García-Rodeja, E., Martínez-Cortizas, A., 2013. Five thousand years of atmospheric Ni, Zn, As, and Cd deposition recorded in bogs from NW Iberia: prehistoric and historic anthropogenic contributions. *J. Archaeol. Sci.* 40, 764–777. <https://doi.org/10.1016/j.jas.2012.07.010>.
- Rea, D.K., Ruff, L.J., 1996. Composition and mass flux of sediment entering the world's subduction zones: implications for global sediment budgets, great earthquakes, and volcanism. *Earth Planet. Sci. Lett.* 140, 1–8. [https://doi.org/10.1016/0012-821x\(96\)00036-2](https://doi.org/10.1016/0012-821x(96)00036-2).
- Revels, B.N., Rickli, J., Moura, C.A.V., Vance, D., 2021. Nickel and its isotopes in the Amazon Basin: the impact of the weathering regime and delivery to the oceans. *Geochim. Cosmochim. Acta* 293, 344–364. <https://doi.org/10.1016/j.gca.2020.11.005>.
- Saha, N., Webb, G.E., Zhao, J.X., 2016. Coral skeletal geochemistry as a monitor of inshore water quality. *Sci. Total Environ.* 566–567, 652–684. <https://doi.org/10.1016/j.scitotenv.2016.05.066>.
- Santos-Echeandía, J., Prego, R., Cobelo-García, A., 2005. Copper, nickel, and vanadium in the Western Galician Shelf in early spring after the Prestige catastrophe: is there seawater contamination? *Anal. Bioanal. Chem.* 382, 360–365. <https://doi.org/10.1007/s00216-005-3112-9>.
- Santos-Echeandía, J., Prego, R., Cobelo-García, A., 2008. Influence of the heavy fuel spill from the Prestige tanker wreckage in the overlying seawater column levels of copper, nickel and vanadium (NE Atlantic ocean). *J. Mar. Syst.* 72, 350–357. <https://doi.org/10.1016/j.jmarsys.2006.12.005>.
- Sen, I.S., Peucker-Ehrenbrink, B., 2012. Anthropogenic disturbance of element cycles at the Earth's surface. *Environ. Sci. Technol.* 46, 8601–8609. <https://doi.org/10.1021/ef03201261x>.
- Shamkhani, M.T., 2013. Controlling and Improving the Treatment of Produced Water Using the Six Sigma Methodology for the Iraqi Oil Fields. University of Central Florida, p. 2508, 2004–2019. (<https://stars.library.ucf.edu/etd/2508>).
- Steffy, D.A., Nichols, A.C., Morgan, L.J., Gibbs, R., 2013. Evidence that the deepwater horizon oil spill caused a change in the nickel, chromium, and lead average seasonal concentrations occurring in sea bottom sediment collected from the Eastern Gulf of Mexico continental shelf between the years 2009 and 2011. *Water Air Soil Pollut.* 224, 1756.1–1756.11. <https://doi.org/10.1007/s11270-013-1756-1>.
- Steven, R.E., Sarah, S.H., 1991. Ocean anoxia and the concentrations of molybdenum and vanadium in seawater. *Mar. Chem.* 34, 177–196. [https://doi.org/10.1016/0304-4203\(91\)90002-E](https://doi.org/10.1016/0304-4203(91)90002-E).
- Sunda, W.G., 1989. Trace metal interactions with marine phytoplankton. *Biol. Oceanogr.* 6, 411–442. <https://doi.org/10.1080/01965581.1988.10749543>.
- Sutherland, J., Costa, M., 2002. Nickel. In: Sarkar, B. (Ed.), *Heavy Metals in the Environment*, pp. 147–215. <https://doi.org/10.1201/9780203909300.ch11>.
- Takano, S., Tanimizu, M., Hirata, T., Shin, K.C., Fukami, Y., Suzuki, K., Sohrin, Y., 2017. A simple and rapid method for isotopic analysis of nickel, copper, and zinc in seawater using chelating extraction and anion exchange. *Anal. Chim. Acta* 967, 1–11. <https://doi.org/10.1016/j.aca.2017.03.010>.
- Takano, S., Liao, W.H., Tian, H.A., Huang, K.F., Ho, T.Y., Sohrin, Y., 2020. Sources of particulate Ni and Cu in the water column of the northern South China Sea: evidence from elemental and isotope ratios in aerosols and sinking particles. *Mar. Chem.* 219, 103751. <https://doi.org/10.1016/j.marchem.2020.103751>.
- Tang, D., Kawamura, H., Lee, M.A., Dien, T.V., 2003. Seasonal and spatial distribution of chlorophyll-a concentrations and water conditions in the Gulf of Tonkin, South China Sea. *Remote Sens. Environ.* 85, 475–483. [https://doi.org/10.1016/S0034-4257\(03\)00049-X](https://doi.org/10.1016/S0034-4257(03)00049-X).
- Tao, J., Zhang, L., Cao, J., Zhong, L., Chen, D., Yang, Y., Chen, D., Chen, L., Zhang, Z., Wu, Y., 2017. Source apportionment of PM_{2.5} at urban and suburban areas of the Pearl River Delta region, south China—with emphasis on ship emissions. *Sci. Total Environ.* 574, 1559–1570. <https://doi.org/10.1016/j.scitotenv.2016.08.175>.
- Wang, C., Zou, X., Feng, Z., Hao, Z., Gao, J., 2018. Distribution and transport of heavy metals in estuarine-inner shelf regions of the East China Sea. *Sci. Total Environ.* 644 (10), 298–305. [https://doi.org/10.1016/0278-4343\(85\)90020-2](https://doi.org/10.1016/0278-4343(85)90020-2).
- Wang, M.M., Yuan, M.Y., Su, D.C., 2017. Characteristics of dry and wet deposition of atmospheric heavy metals and their temporal and spatial variation in China. *China Environ. Sci.* 37, 4085–4096. <https://doi.org/10.3969/j.issn.1000-6923.2017.11.010>.
- Wang, X., Chen, B., Wu, G., 2020. Navigation safety status and countermeasures of Weizhou Oilfield Group in Beibu Gulf. *Guangdong Chem.* 47, 101–102.
- Xu, D., Wang, R., Wang, W., Ge, Q., Zhang, W., Chen, L., Chu, F., 2019. Tracing the source of Pb using stable Pb isotope ratios in sediments of eastern Beibu Gulf, South China Sea. *Mar. Pollut. Bull.* 141, 127–136. <https://doi.org/10.1016/j.marpolbul.2019.02.028>.
- Xu, S., Yu, K., Wang, Y., Liu, T., Jiang, W., Wang, S., Chu, M., 2018. Oil spill recorded by skeletal $\delta^{13}\text{C}$ of Porites corals in Weizhou Island, Beibu Gulf, Northern South China Sea. *Estuar. Coast. Shelf Sci.* 207, 338–344. <https://doi.org/10.1016/j.ecss.2018.04.031>.
- Xu, S., Zhang, Z., Yu, K., Huang, X., Chen, H., Qin, Z., Liang, R., 2021. Spatial variations in the trophic status of *Favia palauensis* corals in the South China Sea: insights into their different adaptabilities under contrasting environmental conditions. *Sci. China Earth Sci.* 64 (6), 839–852. <https://doi.org/10.1007/s11430-020-9774-0>.
- Yu, K., Zhao, J., Wei, G., 2005. $\delta^{18}\text{O}$, Sr/Ca and Mg/Ca records of Porites lutea corals from Leizhou Peninsula, northern South China Sea, and their applicability as paleoclimatic indicators. *Palaeogeogr. Palaeoclimatol. Palaeoecol.* 218, 57–73.
- Zhang, X., Chen, J., Lai, Z., Zhai, L., Lin, M., 2017. Analysis of special strong wind and severe rainstorm caused by Typhoon Rammasun in Guangxi, China. *J. Geosci. Environ. Prot.* 5, 235–251. <https://doi.org/10.4236/gep.2017.58019>.
- Zhao, J., Zhang, Y., Xu, H., Tao, S., Wang, R., Yu, Q., et al., 2021. Trace elements from ocean-going vessels in East Asia: vanadium and nickel emissions and their impacts on air quality. *J. Geophys. Res. Atmos.* 126 e2020JD033984.
- Zhao, X., Xu, C., Shi, Q., 2015. Porphyrins in heavy petroleum: a review. *Structure and Modeling of Complex Petroleum Mixtures*, pp. 39–70. https://doi.org/10.1007/430_2015_189.
- Zhao, Y.Y., Jiang, R.H., Yan, M.C., 1995. Abundance of chemical elements in continental shelf sediment of China. *Geo-Mar. Lett.* 15, 71–76. <https://doi.org/10.1007/bf01275409>.
- Zhong, Q., Pan, Q.Y., 1997. Discovery of offshore oil fields in the northern Beibu Gulf. *Geol. Guangxi* 02, 59–64.